A HIGH SPEED EDGEWISE ROTOR USING CIRCULATION CONTROL ONLY IN THE REVERSED FLOW AREA

I.C. Cheeseman and M.M.E. Soliman**

University of Southampton, UK

ABSTRACT

The application of circulation control by blowing to edgewise rotors has been extensively investigated. Sufficient hardware has been constructed, principally in the USA, to conclude that the basic technology has been proved.

Original circulation control applications were to stopped rotor aircraft which had higher productivity, to compensate for the increased complexity, and slightly lower disposable load relative to the conventional helicopter. The X-Wing was the most advanced and technologically challenging project attempted.

Ten years ago it was realised at Southampton University that a thrust compounded helicopter fitted with a conventional bladed rotor adapted to utilise circulation control in the reversed flow region, might offer substantial performance improvements with relatively little technological risk. This paper describes that programme of work.

To apply circulation control there must be no sharp trailing edge. An aerofoil flying backwards has just such a feature: this is what is normally the leading edge. Blowing slot(s) have been inserted in the nose which do not affect the aerofoil's normal performance. Circulation control can therefore be combined with any advanced aerofoil or blade planform in order to provide positive and significant lift in the reversed flow region.

To calculate the performance of such a rotor it was necessary to determine the aerofoil performance of a typical modern blade section fitted with leading edge circulation control. A wind tunnel model was constructed with a chord equal to that of a typical helicopter main rotor blade. To assist in positioning the slots on the aerofoil, the circulation control jet flow was modelled by the free vortex technique previously reported. A data file of two-dimensional lift, drag and pitching moment was produced which was used in the rotor performance program.

Using RAE generated data for the aerofoil(s) operating normally, a helicopter's performance was satisfactorily predicted. This program was then adapted to allow for reversed flow region circulation control as well as having provision for auxilliary propulsive thrust to be applied. The rotor advancing blade Mach number was not permitted to exceed that used by the conventional rotor.

The results showed that the normal rotor when 'equipped' with circulation control in the reversed flow area could support the helicopter up to 340 knots, this being the maximum speed at which calculations were made. A speed band where the excess rotor thrust to weight ratio was a minimum occurred just above the maximum speed of the conventional helicopter. However, above that relatively small speed range the excess thrust to weight ratio increased significantly. Power for circulation control was minimal, the power required being totally dominated by that required to

** *Now at the Royal Aerospace Establishment, Farnborough*

overcome the fuselage drag which was unchanged from the conventional design. No unusual rotor dynamic problems were detected.

1.0 INTRODUCTION

Circulation control by blowing was developed in the United Kingdom at the National Gas Turbine Establishment, Pyestock between 1958 and 1970. Independently, NASA Langley Field investigated the same technology at about the same time. In both places the objective was the same, namely to produce high lift coefficients using air injected into the boundary layer to alter the position of the separation points. The efficiency of the system in terms of the compressor power required for a given lift coefficient was important. The early work has been summarised in references 1 and 2 which also explain why the original applications suggested at the two establishments were totally different.

Many applications for circulation control have been examined. These include using retractable blown circular cylinders at the nose of a transport aircraft to provide trim forces during take-off and landing, an alternative to flap blowing on carrier borne aircraft and several rotary wing applications.

The original rotary wing application of circulation control at Pyestock was to a stopped rotor transport aircraft aimed at the short haul market. For this aircraft, circulation control allowed the use of essentially circular cross section blades which are largely gust insensitive when no blowing is applied. The thickness/chord ratio of unity of that section gives high flapping stiffness which is useful during the blade stopping manoeuvre. Although initial consideration was given to the attractive idea of using the stopped blades as fixed wings this was rejected due to the difficulty of avoiding undesirably high vibration in the final phases of stopping the rotor. During this phase of the flight the rotor has to maintain lift equal to aircraft weight and produce adequate control moments. This concept has been well researched in the United States and an indication of the extensive work led by R.M. Williams may be gained from references 3 and 8. The earlier work at the NGTE is summarised in reference 5.

The advantages of circulation control to conventional rotors were considered in reference 1. Given a symmetrical blade section, for example an ellipse, blowing can be applied to either the leading or trailing edge in the reversed and normal flow area respectively. It was shown in that paper that it was possible to produce adequate lift and control power to support a helicopter up to an advance ratio of 1.2. It was assumed that the rotor was slowed to minimise advancing blade problems and that auxilliary thrust was provided to overcome drag. This work was extended in the USA and has been reported for example in reference 3. These concepts will be further discussed in section 2.

Other applications of circulation control include the 'Notar' tail rotor concept developed by McDonald Douglas and recently discussed in reference 6. The origin of this idea may be found in reference 7.

Re-examination of the work reported in references 1, 3 and 8 was made at the University of Southampton about ten years ago. It was realised that a more efficient helicopter rotor system could be devised which would offer similar performance advantages simply by using conventional blade sections and limiting the blowing to the reversed flow region. This is possible because conventional aerofoils have rounded leading edges, which in the reversed flow region are the aerodynamic trailing edges. Thus circulation control by blowing can be applied. This paper examines the viability of such a concept.

2.0 THE HIGH SPEED ROTOR CONCEPT

The starting point of the current work was that discussed in reference 1. That paper postulated a rotor fitted with elliptic section blades which had a thickness/chord ratio which varied form 20% at the root to 10% at the tip. These blades were fitted with blowing slots both at the leading and trailing edges. The blowing was automatically transferred from the leading to the trailing edge in the reversed flow region. Since the lift produced by the elliptic section had two components, one due to incidence and the other from blowing, the rotor only had a mechanical collective pitch control, cyclic lift changes being produced entirely by variation of the blowing flow as the rotor rotated.

To assess any penalties which such a rotor system might have, a comparison was made with a conventional rotor of similar dimensions and performance to that fitted to the Westland Wessex. The ability to produce high lift coefficients allows a smaller blade chord to be used. The lift coefficient is related to the blowing momentum required and this requires power to be applied to compress and to pump the air along the blades. Figure 1 taken from reference 1 shows that for the 'equivalent Wessex' rotor if all the lift is produced by circulation control, the power required is twice the conventional rotor profile power. A solution was found by tapering the blade and using some incidence lift. Using the conventional blade chord at the the root but tapering to half that chord at the tip, the hover performance of the two rotors was virtually identical when 5/12 of the lift was produced by blowing, the balance being generated by incidence. The fraction of 5/12 was dictated by the need to maintain adequate cyclic pitch control. It was necessary to increase this fraction as forward speed was increased. Figure 2, from reference 1, shows that the rotor-only power peaked at $\mu \approx 0.8$ when the disc is trimmed to be horizontal, forward propulsion being provided by a separate unit. The reduction in incidence lift is indicated by the decrease in collective pitch required. Work at the David Taylor Naval Ship Research & Development Center, quoted from reference 8 in reference 9, shows that with more developed elliptic blade sections, the peak power occurs at $\mu \approx 0.7$. Figure 1 shows that the compression power dominates the total power required. The reduction of the compression power is clearly shown to be a crucial objective for a successful increased speed rotorcraft.

An important conclusion from this work is that a rotor capable of supporting a thrust compounded helicopter to advance ratios in excess of unity can be made using circulation control by blowing.

Further examination of the work discussed above shows that most of the compression power is being expended on lift generation on the advancing blade. A short reflection leads to the conclusion that any conventional aerofoil could be used there, the blowing is only needed on the retreating side and there only in the reversed flow region. It is then only a short step to note that in the reversed flow area the 'aerodynamic trailing edge' is the normal leading edge which has a rounded profile and is therefore suited to the application of circulation control.

The rotor concept which then emerges is of a conventionally bladed layout fitted with both cyclic and collective pitch controls. The blade section and planform are selected to optimise the performance on the advancing side of the rotor. A circulation control slot is inserted along the upper surface of the blade blowing towards the leading edge. Air is only provided to this slot over an azimuth range $180° \leq \psi \leq 360°$. Auxilliary thrust is provided for speeds above those attained by conventional helicopters. To develop this concept it was necessary to determine the performance in reversed flow of a typical conventional aerofoil fitted for circulation control by blowing.

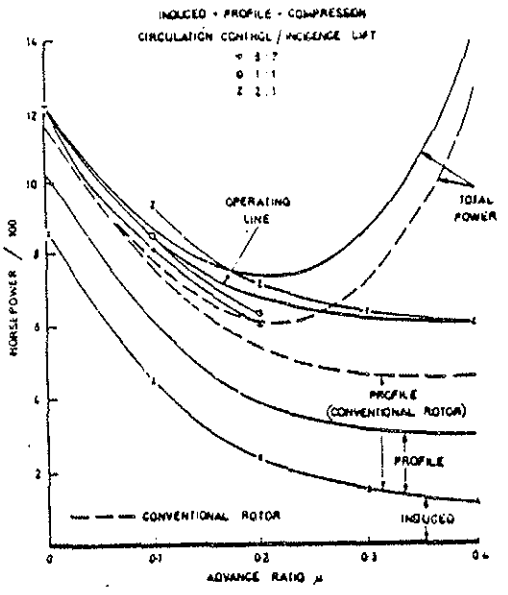

Figure 1
Forward flight performance of simple rotor

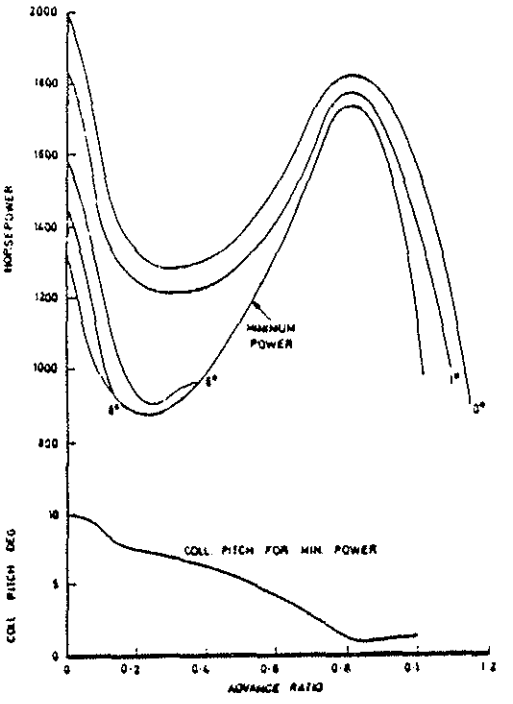

Figure 2
Forward flight performance of advanced rotor with disc horizontal

3.0 SECTION PERFORMANCE OF A BLOWN AEROFOIL IN REVERSED FLOW.

Following discussions with the Royal Aerospace Establishment and Westland Helicopters Ltd. it was decided to concentrate the work on a Lynx size helicopter. The University readily agreed to that suggestion because a successful demonstration at Lynx scale would be an indication of the general applicability of the concept, it having been found that it is easier to apply blowing to large scale rotors. It was therefore natural to use an RAE 9615 aerofoil for the wind tunnel tests, although for practical reasons the thickness/chord ratio was increased to 15%. The tests were made in the 2.1 × 1.5 m working section of the University low speed wind tunnel. The model, which spanned the working section from top to bottom, was constructed with a chord of 50.8 cms, which is larger than full scale for the Lynx so avoiding the need to make any allowance for the Reynolds Number.

The only question which required to be answered before the model could be constructed was the position of the slot or slots. In order to have an indication of the slot position, the theoretical model of circulation control developed at the University and reported in reference 10 was used. Figure 3 shows the free vortex representation of the jet flow developing on a circular cylinder. This showed that, for a 15% t/c symmetrical aerofoil developed by a Zhukovsky transformation, the slot should lie between 24% and 40% of the chord measured from the leading edge, Figure 4. However the theoretical model had slightly overpredicted the performance of earlier reversed blowing aerofoils so it was decided that a better performance might be obtained if the slot was moved nearer to the rounded trailing edge. The possible slot position range was therefore fixed to lie between 18% and 39% chord.

The construction of the model is shown in Figure 5. The trailing edge (used in the conventional flow sense) section was made of wood. The leading edge section, which includes the plenum to supply air to the slot, was made in glass-fibre. The slot

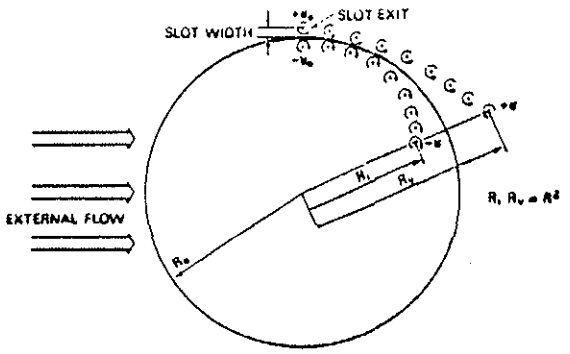

Figure 3
Elements of potential flow model

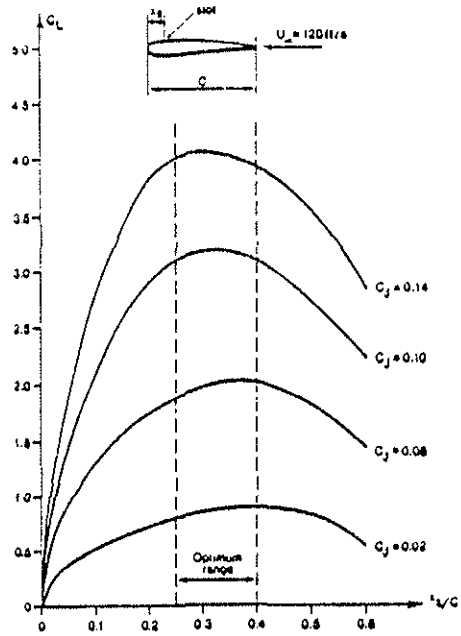

Figure 4
The optimum range of slot positions as predicted by the discrete-vortex model

was constructed by arranging two plates to form the top of the plenum. The gap between these plates formed the slot, the width of which was adjusted by slight fore and aft movement of the plates. This arrangement is shown in Figure 5a. Each plate was screwed to six ribs equally spaced along the span and into the end fixings. To move the slot in a chordwise direction, new pairs of plates were constructed to cover the plenum. Plates were made which allowed the slot to be placed at 0.18, 0.215, 0.25, 0.285, 0.32, 0.355 and 0.39% of the chord. The model was fitted with 37 static pressure tappings arranged around the centre section.

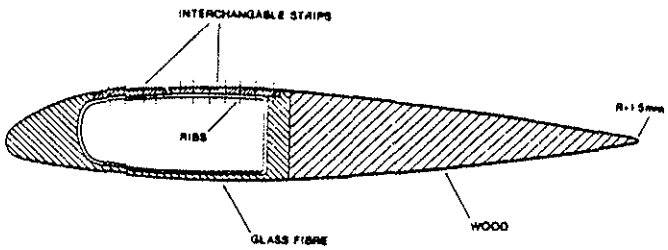

Figure 5
A cross-section of the experimental model

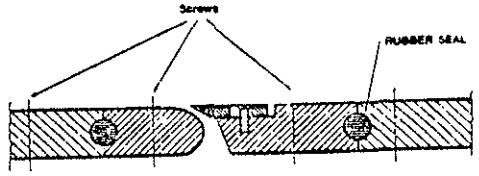

Figure 5a
A cross-section of the two strips which form the slot

A preliminary series of tests was conducted to find the slot position for the optimum lift performance per unit jet momentum coefficient. The results for a tunnel speed of 24 m/s and zero incidence are shown in Figure 6. The optimum performance moves with slot position, at low C_J the best result occurs at 21.5% but at high C_J it is slightly better at 25% chord. Tests at other speeds and incidences

confirmed this general pattern so it was decided to fix the slot for a comprehensive series of tests at 21.5%. The performance variation with slot width was also considered and it was fixed at 0.64 mm. The ratio of slot width/chord = 0.00126 compares favourably with that found by Dunham in his work at NGTE.

The model was tested in wind speeds between 12 and 36 m/s and over the incidence range of 0 to -20°. This negative incidence range was selected to cover all the rotor cases for which useful lift contributions could be produced in the reversed flow region. Lift and pitching moment was deduced from the pressure tappings arranged around the centre section of the model. Drag was determined from wake pressure measurements.

The resultant forces on the aerofoil were expressed as C_N which was normal to the chord and C_H along the line of the chord. These were calculated by resolving the integrated pressure force normal to the chord and the force along the incident flow direction deduced from the wake pressure measurements. An example of the C_N results is shown in Figure 7 which also shows a sample calculation using the vortex model of reference 10. For use in the helicopter rotor analysis, the contribution to total C_N due to circulation control was required. This was obtained by subtracting the unblown value of C_N and labelling the remainder ΔC_N. The normal force magnification factor $\Delta C_N/C_J$ is plotted against C_J in Figure 8 for all tunnel speeds. An acceptable collapse of the data is shown. Since it is easier to visualise the force along the velocity vector C_D than C_H, this is shown in Figure 9. The conversion of a drag into a net thrust as C_J is increased is typical of circulation control applications.

The data produced by these tests were analysed to give the increase in force coefficient and the angle of that force to the normal to the aerofoil chord due to circulation control C_J for any incident flow angle above -20°. This force data could then be resolved into the rotor co-ordinates and added to the forces generated by the unblown aerofoil.

The pitching moment which would be generated by the application of circulation control was a matter of concern at the start of this project. If the resulting centre of pressure approximated to the relevant quarter chord (3/4 chord in the conventional sense) then the total blade pitching moment for the control system to react could be excessive. From the measured pressure distributions the position of the centre of pressure was determined and expressed as a fraction of the chord from the conventional leading edge. The results are shown in Figure 10. It is clear that there is unlikely to be a problem.

On completion of this section of the programme it was clear that:

1) Circulation control produced substantial positive lift on a conventional aerofoil in reversed flow at incidences down to -20°.

2) The centre of pressure of the section forces was in the vicinity of the conventional 1/4 chord point and was therefore unlikely to produce torsional problems and excessively high blade control moments.

4.0 THE CALCULATION OF THE PERFORMANCE OF A HELICOPTER EQUIPPED WITH A REVERSED FLOW CIRCULATION CONTROL ROTOR.

4.1 General

Section 3 explained the reason why the principle of the reversed flow rotor was being applied to a Lynx-like helicopter modified as required for the higher speed. The important parameters of the Lynx are shown in Table 1. For all the results given

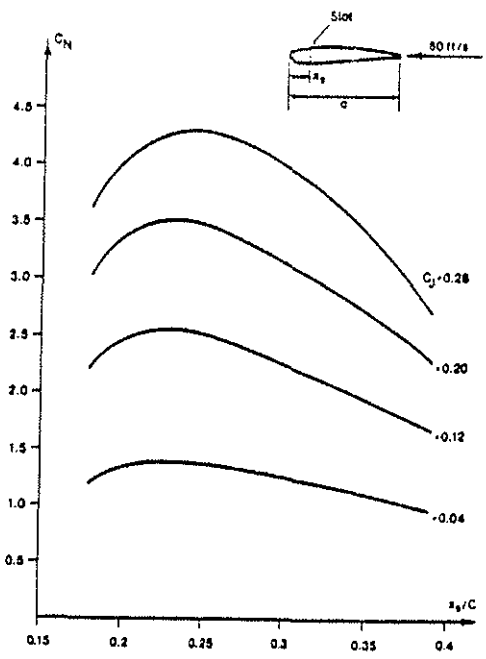

Figure 6
The experimental optimization of slot position

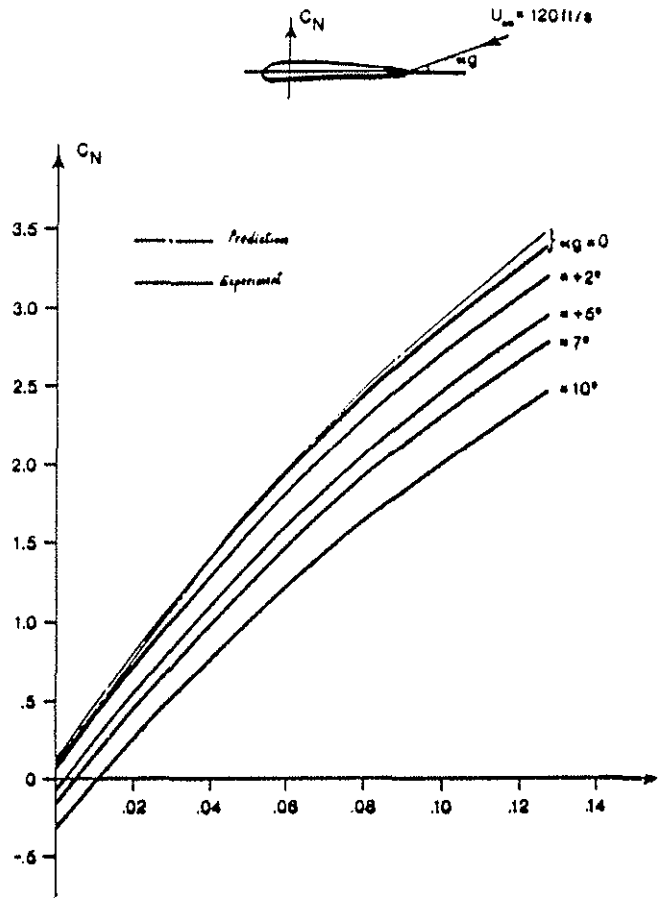

Figure 7
Variation of normal force coefficient with jet momentum and incidence U_∞ = 120ft/sec

in this paper these parameters were used. The data was provided by RAE and Westlands.

Table 1
Lynx-like Parameters used in the Assessment

AUW = 40 KN
Angular velocity Ω = 33.3 rad/s
Blade chord c = 0.394 m
Hub cut-out/R = 0.15
Hub drag coefficient = 0.25

Rotor Radius R = 6.401m
Number of blades b = 4
Blade twist θ_{tw} = 4.5°
Pseudo flapping hinge offset/R = 0.1

The fuselage lift, drag and pitching moment coefficients were provided as look-up tables for different pitch attitudes. A non-specified auxilliary propulsion unit was assumed to be attached to the fuselage to propel the machine above normal helicopter speeds. The power used by this unit was calculated assuming an efficiency of 75%.

4.2 Isolated Rotor Performance Calculation

The rotor blades were assumed to be modified with a slot inserted similar to that shown in Figure 5. It was assumed that compressed air is produced and

delivered to the blades through a valve arrangement such as that used in reference 5, Figure 11, a generally similar unit being used in reference 4. The slot width was assumed to be constant along the blade span. Experience has shown that centrifugal compression approximately balances the duct pressure losses. The jet momentum emerging per unit span was calculated at each spanwise location. Thus the local jet momentum coefficient was evaluated and the actual lift increment generated by this blowing was found by reference to a look-up table produced from the aerofoil wind tunnel data discussed in section 3. To complete the calculation of the blowing performance the power and duct size had to be assessed. The duct area was checked for compatability with the blade cross-section. The maximum duct flow velocity was Mach 0.4. The pressure losses in the compressor and the ducting were assumed to be 20%. The pumping power required to supply the angular momentum to the mass flow as it flowed along the blade was calculated separately. The blade slot was assumed to be convergent so the emergent velocity was restricted to Mach 1. Therefore it was not efficient to use a slot pressure ratio greater than 1.89 and all results quoted here satisfy this condition.

Early work showed that, even with a 'rigid' blade approximation, it was important to estimate accurately the flapping motion. The usual blade flapping equation for the case of an offset flapping hinge, either real or equivalent for a semi-rigid rotor, was used. The flapping angle β was assumed to be small. The rotor equations were developed relative to the non-feathering plane. The Glauert induced velocity distribution was assumed. While the equations are well known and have previously been solved, because this work was extending the solution to higher advance ratios, it was assumed that flapping coefficients higher than the first must be included. Two basic classes of solution exist. The harmonic method, developed by Gessow in 1956 and modified by Johnson, estimates the flapping motion at a number of azimuthal positions so allowing evaluation of the blade hinge aerodynamic pitching moment. This pitching moment is expressed as a Fourier series and the flapping differential equation is solved analytically by equating the coefficients of each harmonic to find new estimates of the blade flapping coefficients. The process is repeated until the values of the flapping coefficients converge to a prescribed accuracy. The alternative numerical solution method estimates the aerodynamic moment as above but then integrates the differential equation numerically by azimuthal steps. The iteration stops when the blade flapping coefficients for successive rotor revolutions agree to a prescribed accuracy. It was decided to follow the harmonic approach as there was no immediate requirement to predict rotor transient behaviour. Dr Soliman's method of solution proved to be computer efficient as well as being easily extended to elastic blades and was as follows.

Initial values of the flapping coefficients (a_n, b_n) were assumed which gave numerical expressions for β, $d\beta/d\psi$ and $d^2\beta/d\psi^2$. The aerodynamic moment was then evaluated by integrating numerically along the blade span at a number of azimuthal positions equal to the number of flapping coefficients. Subtracting the inertia and centrifugal moment should produce zero moment at the flapping hinge but in general the first approximation resulted in a non-zero 'error' value. A well proven minimisation of error technique was applied and this often produced convergence within three iterations.

The calculation of the aerodynamic forces was made in the usual manner except that no approximations were made to the expression for the local velocity and incidence. The usual appoximations and the more exact calculations gave good agreement up to $\mu = 0.4$ but significant differences were found above that advance ratio.

The output from this sub-routine gave the hub forces and moments which were then integrated into the overall helicopter performance and trim calculations.

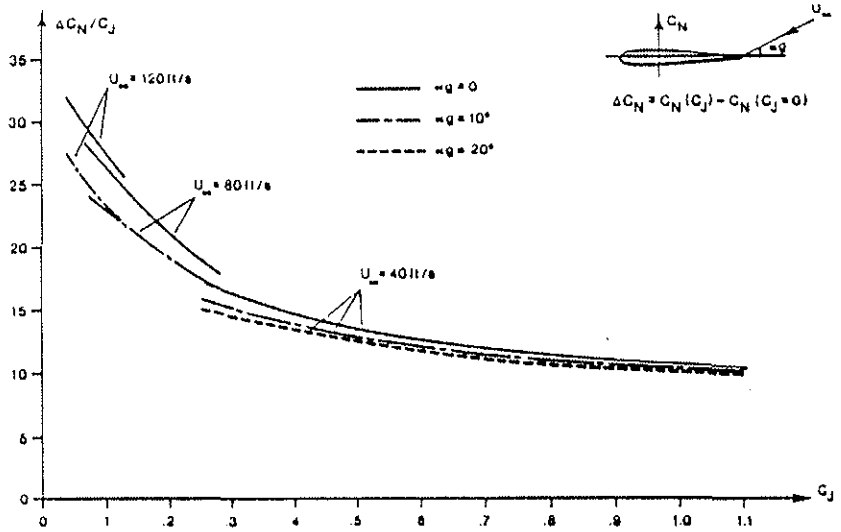

Figure 8
Jet Efficiency

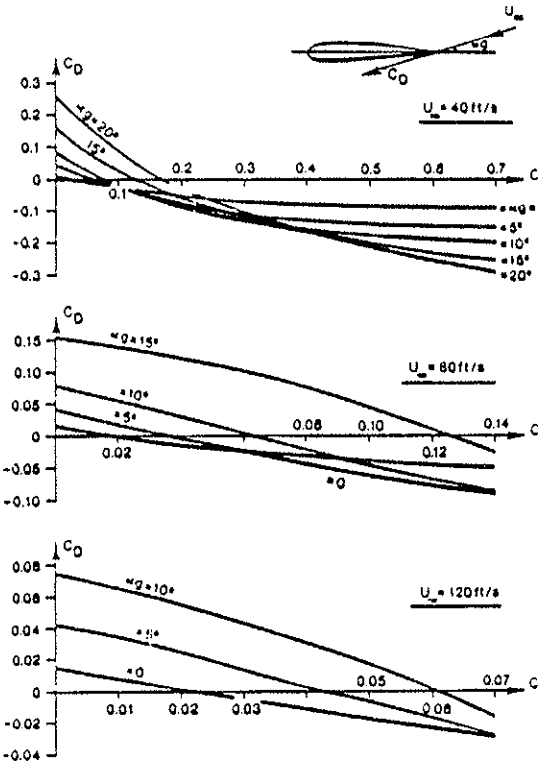

Figure 9
Variation of drag coefficient with jet momentum, incidence and freestream velocity

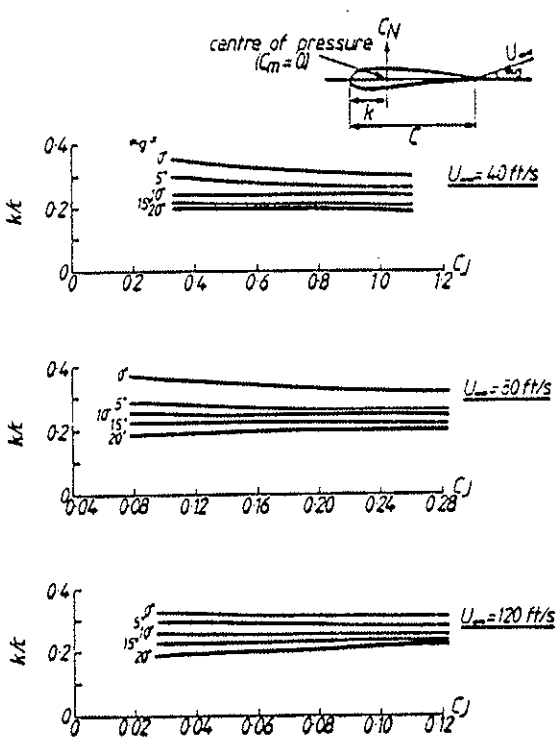

Figure 10
Variation of the centre of pressure at different incidences, freestream velocities and momentum coefficients.

4.3 Complete Helicopter Trim and Performance Calculation

The helicopter was trimmed in all planes. The overall forces and moments in the longtitudinal plane are shown in Figure 12. The similar diagram for the lateral plane is not shown because the only extra force to be included is due to the tail rotor. The program was run for an operator-entered forward speed, slot pressure ratio, auxilliary thrust/fuselage drag ratio, auxilliary thrust inclination and location (fore and aft and vertically from the hub) and point of application of the fuselage aerodynamic forces. The slot pressure ratio was assumed constant throughout the reversed flow region although it was realised that there would be a gain in slot air compression power if, as can be seen to be practical from Figure 11, the pressure was varied azimuthally and possibly spanwise. However, as will be shown, the compression power is such a minor contributor to the total power that this additional program complication was deemed not to be cost effective. Figure 13 is the schematic of the program. The program assumed a fuselage attitude and values for the collective and cyclic pitch and the flapping coefficients, either from a default or from the last case calculated. The various parameters were then adjusted in the program until the vertical force equalled the weight and the horizontal and side forces, overall pitch, roll and yawing moments were zero, each to its own pre-set accuracy. Yawing moment was compensated by a force situated at the same position as, and with a similar performance to the Lynx tail rotor.

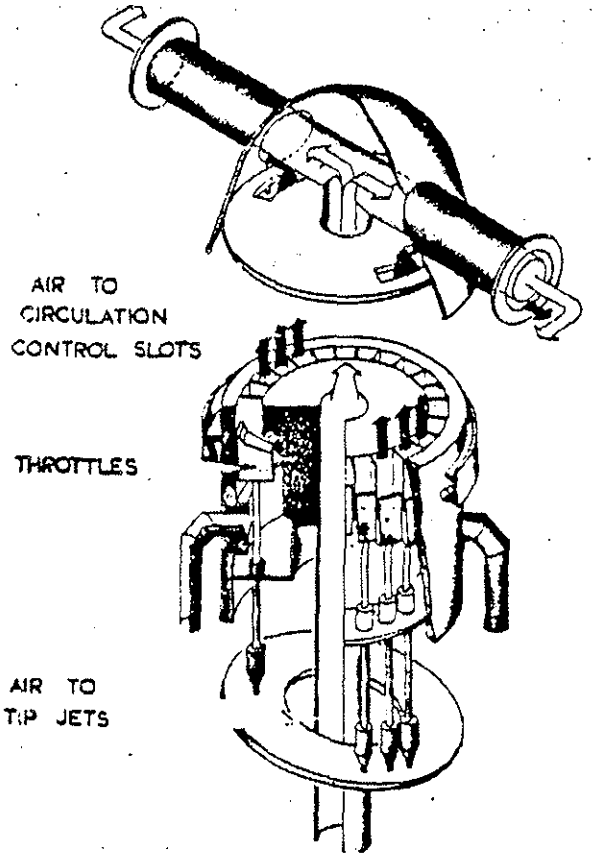

Figure 11
Circulation controlled rotor cyclic control hub

The program could be run with the rotor operating at a fixed angular velocity. Alternatively the program could reduce the angular velocity so that the advancing blade tip velocity remained constant after a predetermined value was reached, normally the speed giving a Mach number of 0.95.

Some results obtained from these programs are discussed in the next section.

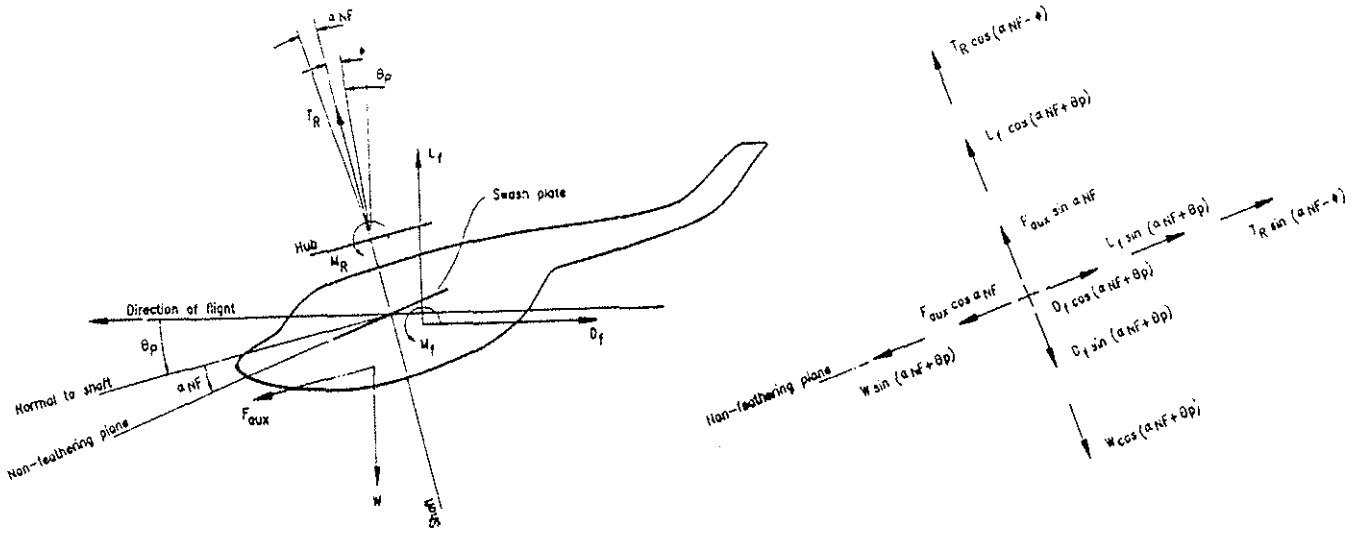

Figure 12
The force components acting on a helicopter

5.0 ISOLATED ROTOR AND COMPLETE HELICOPTER PERFORMANCE

5.1 Isolated Rotor Performance

This section reports calculations made for an isolated rotor in horizontal flight at a range of shaft tilts. The cyclic pitch was chosen so that the resultant rotor force was along the rotor shaft. The results are presented in Figure 14 for three shaft tilts of 0°, -3° and -6° (negative values indicate nose up tilt) as values of C_{Tmax}/S versus μ. The definition of $C_{T\,max}/S$ is:

$$\frac{C_{Tmax}}{S} = \frac{T_{max}}{\frac{1}{2}\rho b c R V_T^2}$$

where the symbols have their usual meaning with one exception. V_T is the rotor tip speed in the hover which is not necessarily that in use at the value of μ under investigation. As a point of reference the hover value of C_T/S for a lift of 40 kN is 0.132. The fourth curve is for the same rotor at a shaft tilt of 0° but with no circulation control applied. This curve is not bettered for the unblown rotor for more negative shaft tilts. The contribution of the circulation control to overall lift as nose tilt is increased is clear from this figure.

Comparing the curves for shaft tilts of -3° and -6° in Figure 14 shows that above a certain shaft tilt the RFCC (Reversed Flow Circulation Control) rotor produces a minimum lift at about μ = 0.8. This result is in close agreement with the earlier results reported in references 1 and 8. Making the shaft tilt more negative increases the value $C_{T\,max}/S$ above the value for -6° while retaining the shape of that curve including the position of the minimum.

The curve for -6° in Figure 14 shows that the 40 kN helicopter could just be supported through the speed range by the rotor alone. Excess thrust for control could be produced by an increase in rearward shaft tilt. It will be obvious that, since the shaft is inclined rearwards, a normal rotor installation will result in some fuselage lift being produced. Thus the final fuselage attitude for a complete helicopter will be less than the 6° nose up at about μ = 0.8 implied by Figure 14. The design of the

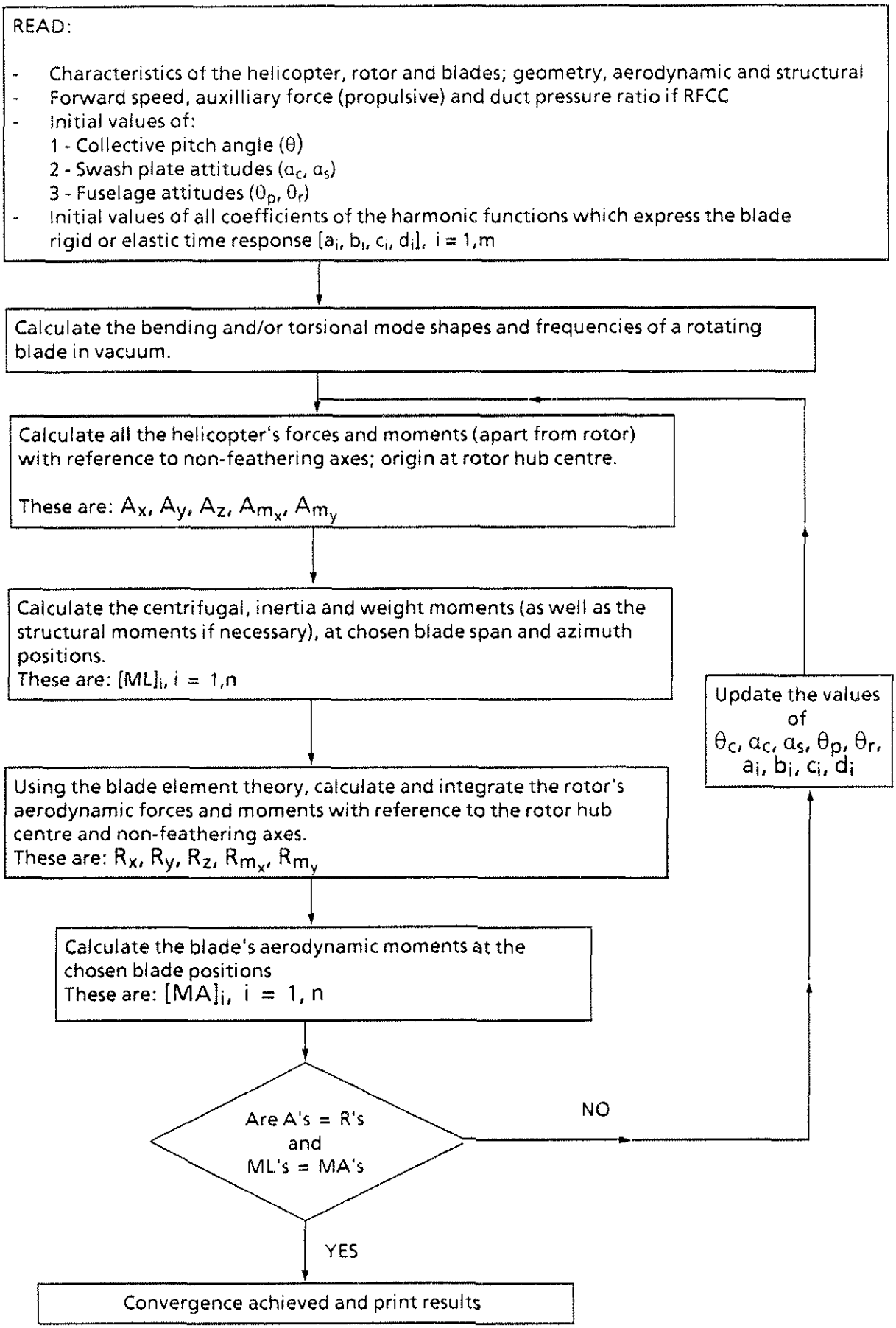

Figure 13 - Program flow diagram

fuselage to produce lift without high drag is likely to be an aim for any high speed helicopter design.

The curve for a shaft tilt of -6° at μ = 1.0 has a positive gradient and calculations up to μ = 2.0 have shown that this upward trend is continued. This effect is not a surprise, for the difference in dynamic heads on the advancing and retreating sides of the disc reduces as μ increases above μ = 1.0

An ab-initio rotor design must address the rotor design compromise which arises due to the requirement for efficient hover and adequate lift to 'pass through the corridor' in the vicinity of μ = 0.8. However the fact that the Lynx-like rotor geometry used for these calculations gave a reasonable result suggests that this compromise may not be difficult to find.

The rotor not only produces lift, it produces drag and absorbs power. It is instructive to look at the lift/drag ratio of the isolated rotor since this figure can then be contrasted with the equivalent value of the ratio for other lifting devices, like the fuselage. It is therefore necessary to define the equivalent drag of the rotor, the lift value being self-evident. It should be noted that these values are quoted for an isolated rotor which had been trimmed to produce a force which was directed along the rotor shaft. Hub pitching and rolling moments were generally not zero.

The lift L was the component of the thrust T normal to the flight vector.

The equivalent drag D was composed of two terms.

The first, H, was the component of the thrust along the flight direction (+ve to the rear).

The second term, D_P, was the (rotor power + Circulation Control power)/(forward speed).

Thus $D = H + (P_R + P_{CC})/V$

It will be appreciated that this definition is somewhat unfair to the rotor as it assumes that the power values in D_P are converted to thrust with 100% efficiency. However, rather than embark on a discussion of the efficiency to be applied we have preferred to accept the less good L/D ratios which result from the above definition.

The L/D results for the Lynx-like rotor with and without circulation control are shown in Figure 15 for the same conditions as used in Figure 14. For a given μ the value of $C_{T\,max}/S$ is not the same for each curve as Figure 14 shows. Therefore an additional curve is shown in Figure 15 for the rotor producing a constant C_T/S of 0.132. This curve shows that an L/D of better than 7.5 is predicted. It is considered that this L/D value achieved by a rotor not designed for this high speed, particularly when coupled with the above comments on the assumptions used to convert 'power' to 'drag' is most encouraging.

5.2 The complete RFCC Rotor Helicopter Performance

Using data for a Lynx-like helicopter layout equipped with an unspecified 75% efficient propulsive system and a RFCC rotor, the helicopter was trimmed through the speed range 0 to 340 knots. The auxilliary propulsive thrust was assumed to act along the fuselage waterline through the centre of gravity. No thrust vectoring is included in the calculations presented here. The helicopter was trimmed in all planes.

From the discussion in section 5.1 it will have been appreciated that there is not an unique trim condition at any one speed as the rotor and fuselage attitude and auxilliary thrust are inter-related. The following results are for minimum power

required. A small increase in auxilliary thrust may lead to a condition of minimum blade flapping which, with a semi-rigid rotor hub, may lead to lower stresses and better through life costings.

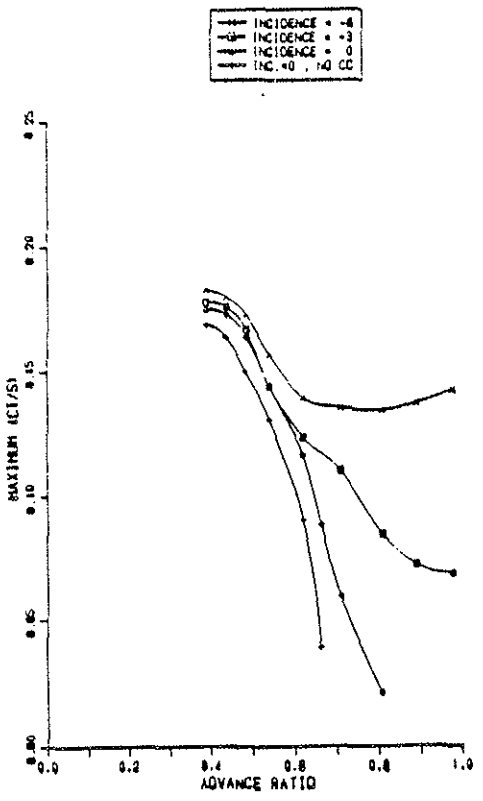

Figure 14
Maximum (CT/S) of an isolated rotor at various nose-up tilts of the shaft

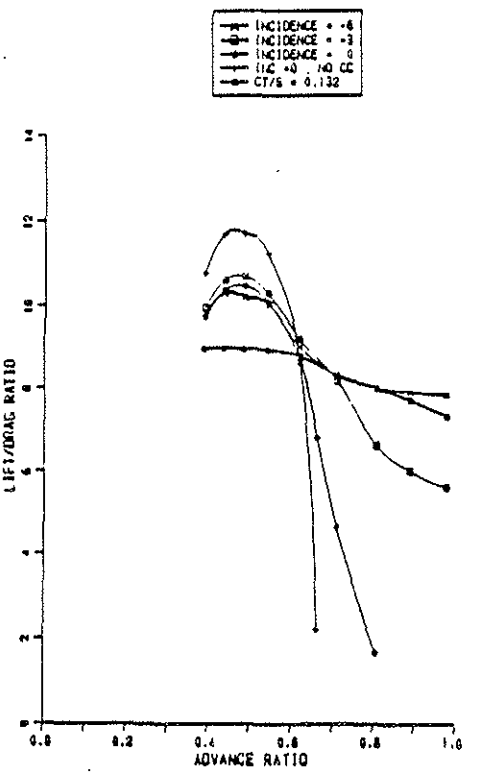

Figure 15
Lift/drag ratios of the isolated rotor at various nose-up tilts of the shaft

The total power required to maintain the helicopter in level flight is shown in Figure 16 together with the component powers. The conversion of advance ratio to forward speed is shown in Figure 17. The values below μ = 0.39 are for conventional rotor propelled flight and show reasonable agreement with Lynx performance on which it is based. For values above that advance ratio Figure 16 shows that the auxilliary power rapidly dominates the total power. Since this power is related to the drag of the Lynx-like design, which was conceived for speeds below 200 knots, the numerical value of the total power is of small importance. What is of greater interest is the value of the magnitude of the auxilliary thrust to the fuselage drag at any speed. This ratio is shown in Figure 18. This shows the drag contribution of the rotor by the amount that the ratio exceeds 1.0. It is clear that for the target cruise speeds of around 300-340 knots ($\mu \approx 1.0$ - 1.25) the increment in auxilliary thrust/fuselage drag above 1.0 is modest. Hence any reduction in fuselage drag will have an important reduction in total power. Assuming no change in fuselage lift and pitching moment, an e% reduction in fuselage drag would produce a decrease of w% of the auxilliary power where

$$w\% = \frac{\text{e\% reduction in fuselage drag}}{\text{Original auxilliary thrust/original fuselage drag}}$$

For example the auxilliary thrust/fuselage drag ratio μ = 1.0 is 1.26 (Figure 18). If a 50% reduction in fuselage drag were to be achieved then w = 39.7%.

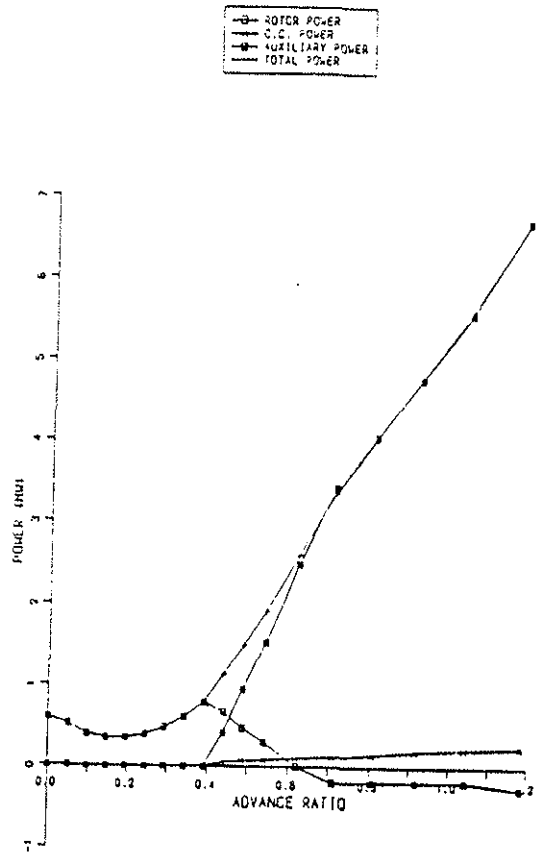

Figure 16
Variation of various components of power with advance ratio

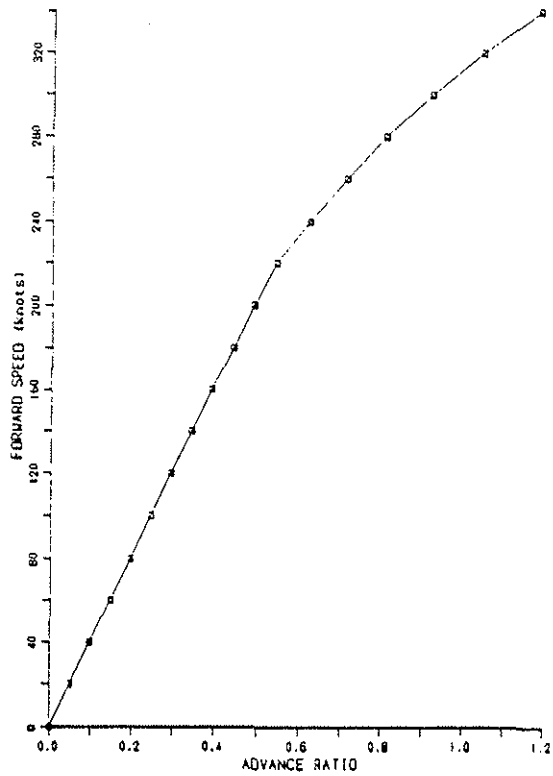

Figure 17
Variation of advance ratio with forward speed

In section 2.0 the relatively large power required by the circulation control air supply of previous designs was mentioned as an important reason for only blowing on the retreating side of the disc. The small contribution made by the CC power in Figure 16 shows that this has been achieved.

The shape of the rotor power contribution shown in Figure 16 was expected. It indicates that the rotor flies in or near to autorotation at the higher speeds.

It is instructive to examine how the lift production is shared around the disc. The lift on a blade, calculated at 24 azimuthal stations, multiplied by the number of blades and divided by the total helicopter weight gives the blade loading. The results of this calculation are shown in Figures 19a and 19b. In both figures the variation in blade loading for the helicopter in conventional flight at $\mu = 0.4$ is shown so that easy comparison can be made with a RFCC helicopter operating at $\mu = 0.7$ (19a) and $\mu = 1.0$ (19b). Figure 19a shows the contribution of circulation control by the maximum in the blade loading curve near to $\psi = 270°$ at $\mu = 0.7$ compared with the $\mu = 0.4$ curve. The blade loading near to $\psi = 90°$ and $270°$ suggests that the lift capability of the advancing and retreating blades are similar. However, Figure 19b shows a different situation. The maximum blade loading during the whole rotor revolution is now produced at $\psi = 270°$ while the advancing side has a roughly constant value. This situation may be remedied by the choice of a different aerofoil section which has improved lift capabilities at high subsonic Mach numbers. The blade in the vicinity of $\psi = 0°$ and $180°$ has the greatest difficulty in providing a reasonable lift contribution and the detailed blade design needs to be examined to improve this situation. It is however reasonable to claim that the RFCC rotor has successfully delayed the 'Advancing - Retreating Blade Performance Trap' of the edgewise rotor to significantly higher speeds.

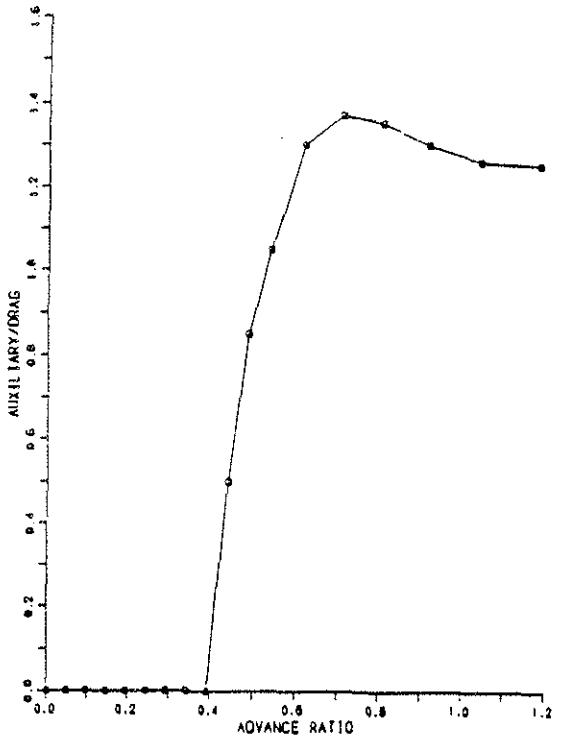

Figure 18
Variation of auxilliary force/fuselage drag ratio with advance ratio

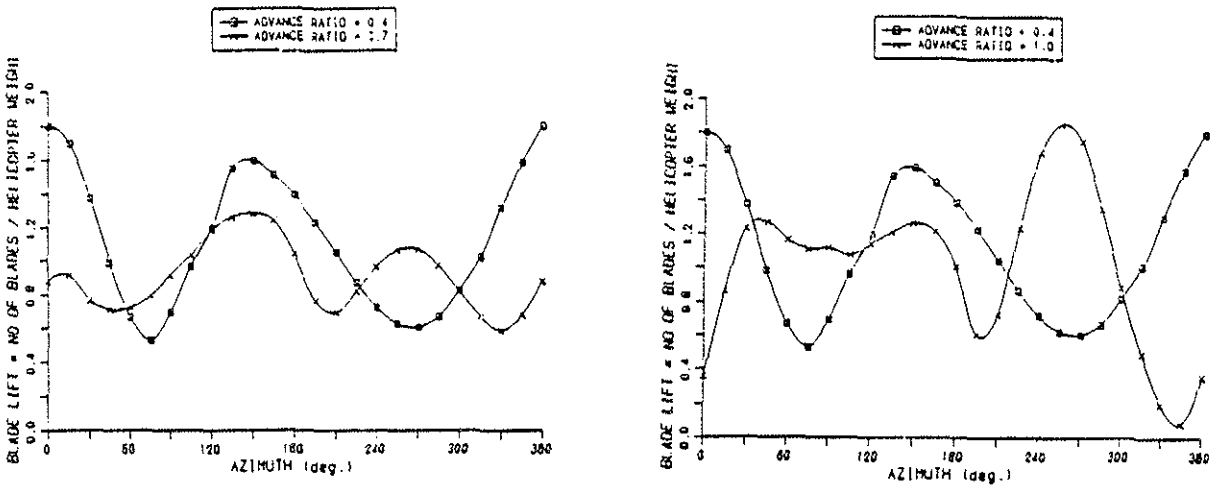

Figure 19
Comparison between azimuthal variation of blade loading at advance ratios
a) 0.4 and 0.7 b) 0.4 and 1.0

The fuselage attitude through the transition is shown in Figure 20. The values shown there were considered acceptable.

This work was made assuming that the rotor had an offset flapping hinge and a rigid blade. Figure 21 shows the maximum rotor flapping angle versus advanced ratio. The maximum blade flapping angle of about 13° at the highest speed was not

considered acceptable and the modelling was changed to that for a semi-rigid hub of the type fitted to the Lynx. This greatly reduced the flapping as will be shown in the next section.

In summary this section has shown that using the characteristics of a Lynx-like helicopter fitted with an auxilliary thrust device:

Practical flight up to a speed of 340 knots can be achieved.

The importance of the fuselage aerodynamic forces have been noted, in particular the need to reduce the fuselage drag.

At the upper end of the speed band the major rotor problems are the generation of sufficient lift on the advancing blade, and at the front and rear of the rotor. This suggests that the choice of aerofoil section(s) and the blade geometry may produce significant improvements in overall performance relative to the figures quoted here.

The maximum blade flapping angles produced at the higher advance ratios for a rotor equipped with an offset flapping hinge and rigid blades are too large. The use of a semi-rigid hub is investigated in the next section of the paper.

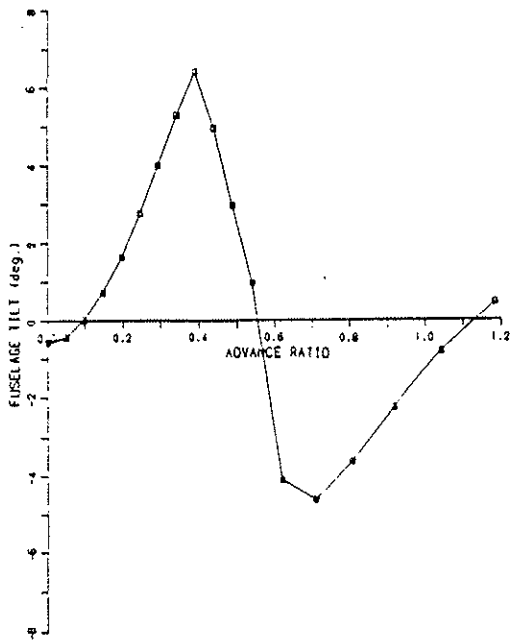

Figure 20
Variation of longitudinal fuselage tilt (positive nose-down) with advance ratio

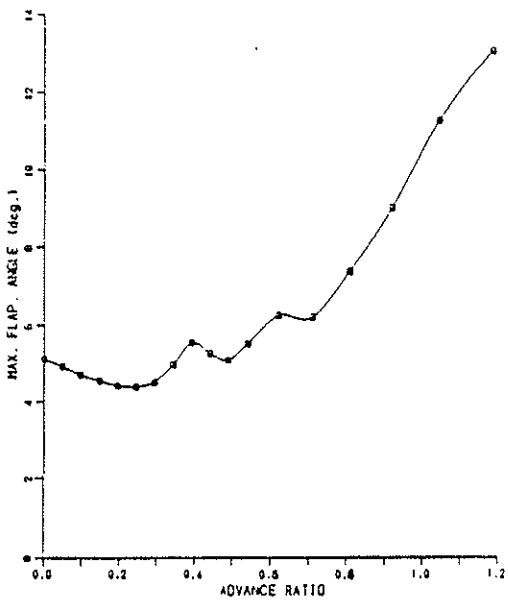

Figure 21
Variation of maximum flapping angle with advance ratio.

6.0 THE EFFECT OF BLADE DYNAMICS ON HELICOPTER PERFORMANCE

6.1 The Modelling of the Blade Flexibility

Section 5 has shown that a rotor equipped with reversed flow blowing produces a performance which can support a typical modern helicopter to speeds of 300+ knots without any other dedicated lifting device. In section 3 the possible problem of large torsional moments was mentioned. These moments may arise due to displacement of the centre of pressure from the blade feathering hinge line when

circulation control is applied. This section examines some aspects of blade flexibility using the characteristics of a Lynx-like rotor including modelling of the semi-rigid hub.

The rotor performance program discussed in section 4 assumed rigid blades. The calculation technique developed by Dr Soliman and outlined in section 4.2 was capable of ready extension to elastic blades. The objective of this phase of the work was to determine the azimuthal variation of the bending and torsional deflection and moments at any advance ratio. The program was therefore extended to calculate the normal modes, blade response and helicopter performance as follows.

The normal modes of the blades, assumed to be rotating in a vacuum, were first calculated. The usual differential equations were derived by requiring the total moment, either bending or torsional, to be in equilibrium at any spanwise position. The bending and torsional displacements were then expressed in the appropiate normal modes. Thus the non-dimensional (with blade length L) bending displacement V(x) is then represented by polynominals in the non-dimensional blade radius X = x/L (where x is distance outboard of the flapping hinge) and the torsional deflection at radius r, T(r), by a series of cosine functions. The expressions used were:

$$V(x) = \sum_{k=1}^{N} \sum_{j=1}^{N+3} S_{j,k} \times X^{j}$$

$$T(r) = \sum_{k=1}^{M} \cos \alpha_{k} (1 - \rho)$$

where N and M are the number of the bending and torsional modes respectively,
$S_{j,k}$ the polynomial coefficient of the j for the 'k'th bending mode,
α_k the coefficient forthe 'k'th torsion mode
and ρ the distance of station r from the shaft/rotor radius R.

Substituting these expansions into the differential equations, the mode shapes and unknown coefficients were calculated by the Galerkin method.

The time history of the blade response was then evaluated by expressing the bending deflection Z and twist θ as Fourier series in ψ, the azimuthal angle, and the appropriate mode shapes as follows:

$$Z(x,\psi) = \sum_{k=1}^{N} \left[V_{k}(x) * \left\{ a_{o,k} + \sum_{i=1}^{m_1} a_{i,k} \cos i\psi + \sum_{i=1}^{m_2} b_{i,k} \sin i\psi \right\} \right]$$

$$\theta(r,\psi) = \sum_{k=1}^{N} \left[T_{k}(r) * \left\{ c_{o,k} + \sum_{i=1}^{m_1} c_{i,k} \cos i\psi + \sum_{i=1}^{m_2} d_{i,k} \sin i\psi \right\} \right]$$

where a,b are the coefficients of the harmonic functions for the time response of each bending mode k

and c,d are the coefficients of the harmonic functions for the time response of each torsional mode k.

The unknowns a, b, c, and d have to be determined. The iterative technique described in section 4.1 has been applied to obtain zero moment at the requisite number of radial and azimuthal stations. The number of points P is determined by

$$P = (m_1 + m_2 + 1) * N$$

for the bending modes equation, the +1 within the bracket accounting for the a_0 term. The P points can be divided between azimuth and radial stations as deemed suitable by the operator. This routine was substituted into the complete helicopter trim suite of programs in place of the rigid blade approximation discussed in section 4.2. The torsional blade freedom was incorporated in a similar manner. The results obtained using the rigid blade approximation and those with three bending and one torsion mode are now compared. It will have been noted that the rotor speed was reduced to restrict the advancing blade tip Mach number to 0.95. The consequent reduction in rotor rotational speed resulted in a lower centrifugal stiffening with consequent change in mode frequency and slight change in shape. The modes were therefore calculated at each rotational velocity used.

6.2 The Effect on Performance

Using stiffness and mass data typical of rotors of the Lynx family of helicopters, the extended complete helicopter performance program was run for the same flight conditions as were discussed in section 5. The helicopter performance results can be summarised by 'very little change in the results given in Figures 14 - 20 was found'. For the rotor control parameters the inclusion of blade bending had negligible effect while blade twist produced only small changes in collective and cyclic pitch settings. These effects were as anticipated.

The blade bending and twist responses are shown in Figures 22 to 25. Figure 22 shows the azimuthal variation of the tip flapping for three bending modes. The results contain no real surprises, the tip deflection being dominated at all speeds by the first mode bending. At the higher speeds of 260 and 340 knots the second mode response changes as expected given the blade loading variations shown in Figure 19 (a and b). Both the second and the third mode remain small for all conditions. No pre-coning of the blade was used in any of these models.

Figure 23 compares the tip flapping for the three bending mode blade model with the value obtained using the rigid blade approximation with offset flapping hinge used in section 5.2. The maximum tip flapping angle is lower for the semi-rigid hub at all speeds. The reduction at a speed of 340 knots is about 60%. The values for the semi-rigid hub were considered acceptable.

It was thought prudent to calculate the maxiumum non-dimensional bending moment in the blade for the semi-rigid attachment. The maximum value occurs at the blade root and the results for the four forward speeds are shown in Figure 24. These show an increase in peak-to-peak value as speed is increased. The variation follows the blade loading patterns shown in Figure 19 (a and b). The need to consider a redesign of the blade profile and choice of aerofoil section to remedy lack of lift production at the front and the rear of the disc as well as the lift limit on the advancing blade made at the end of section 5.2 is equally pertinent here.

The twist arising from torsional deflection at the three forward speeds is shown in Figure 25. The patterns are as expected. Increasing speed from 160 to 260 knots, the largest change occurs on the advancing side with the tip twist altering from a wash-out of 2.8° to a wash-in of about 1.5°. This reflects the changed attitude of the rotor with the result that the spanwise lift distribution along the advancing blade is markedly changed.

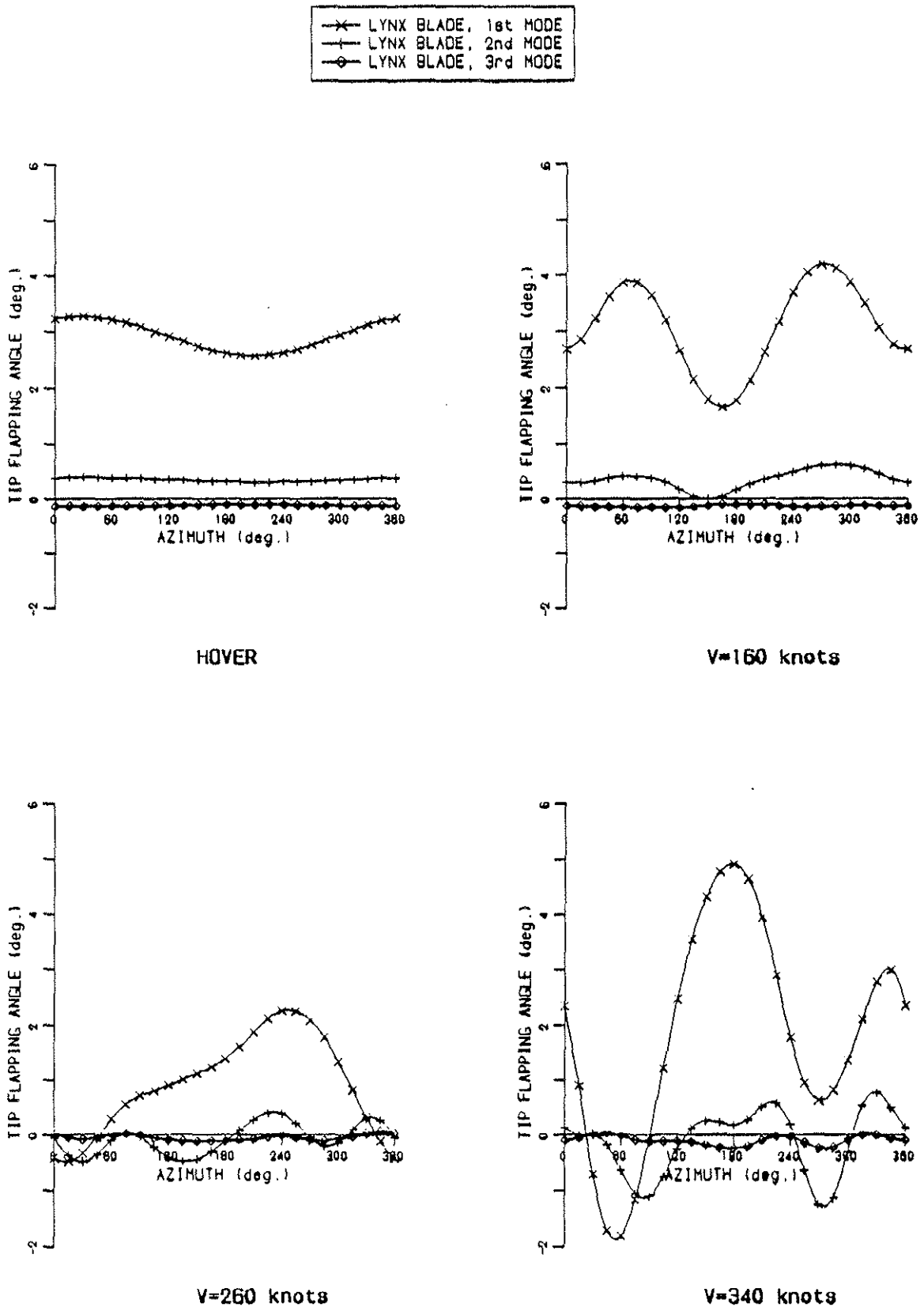

Figure 22
Azimuth variation of tip flapping angles for the three mode shapes of a Lynx type blade

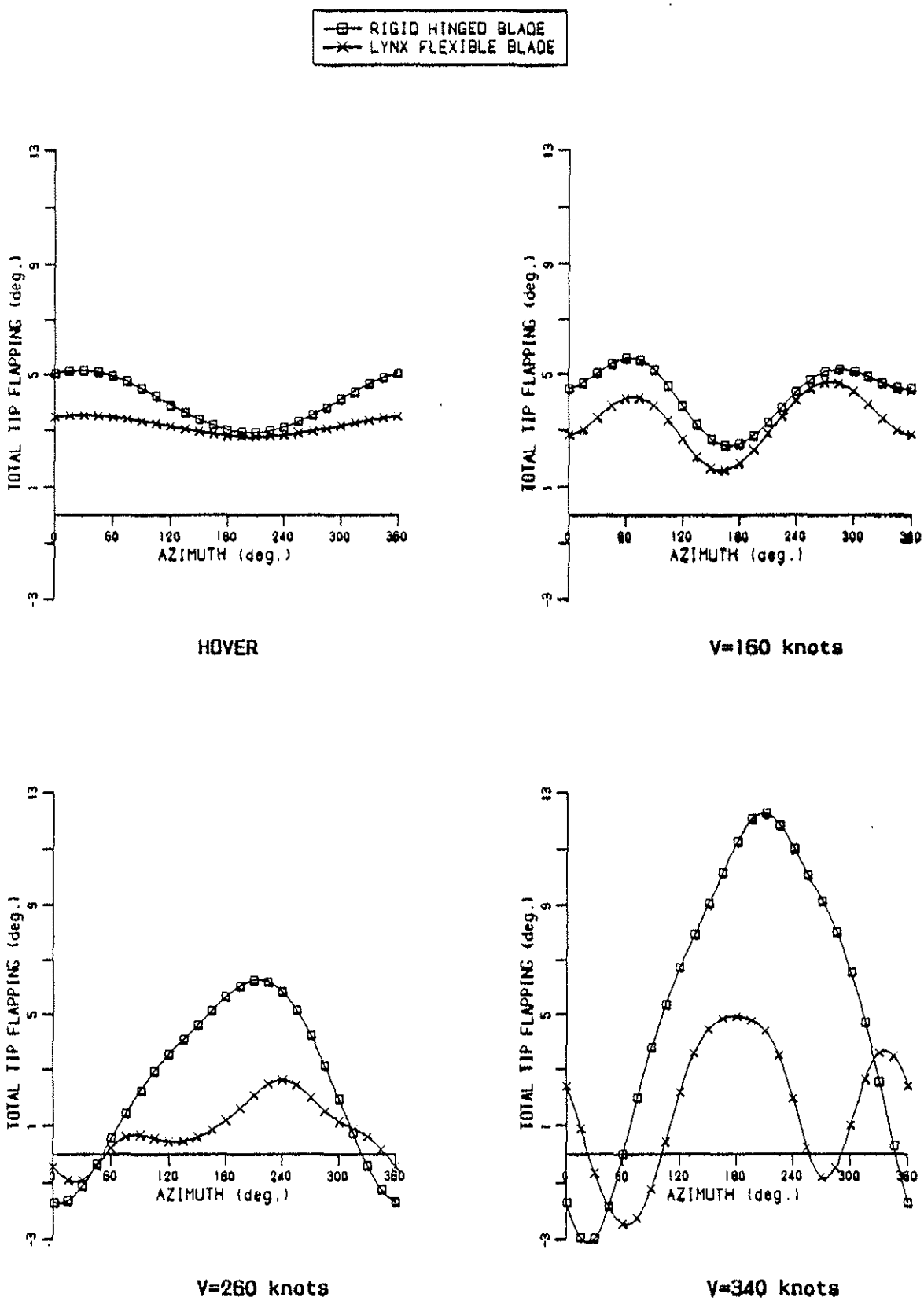

Figure 23
Total flapping angles of a Lynx blade compared to a rigid hinged blade

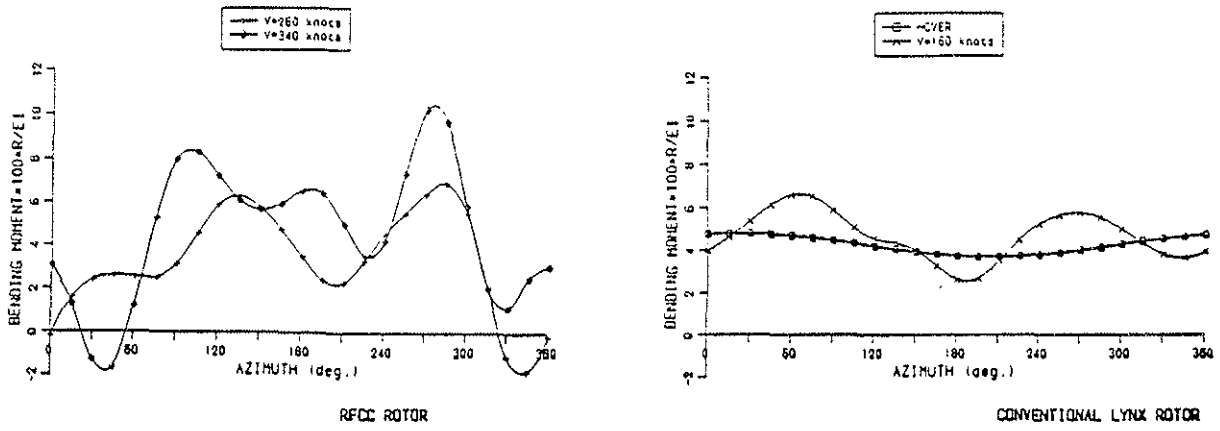

Figure 24
Azimuthal variation of the bending at the Lynx blade root

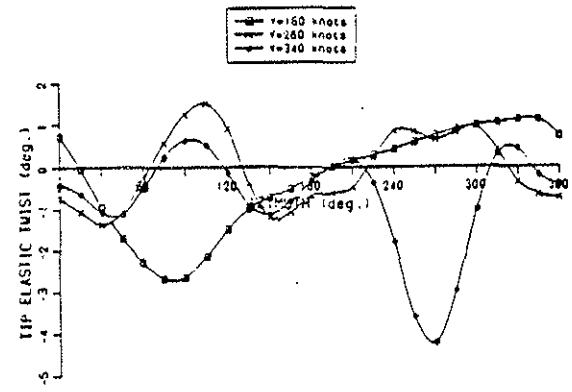

Figure 25
Azimuthal variation of blade elastic twist at various speeds

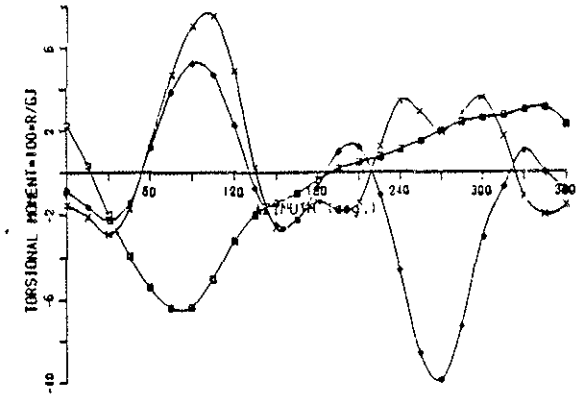

Figure 26
Azimuthal variation of blade root torsional moments

On the retreating side the tip elastic twist is very little changed. This speed corresponds to a μ = 0.8 so the major circulation control moments are acting on the inboard end of the blade. At 340 knots the pattern has changed considerably on the retreating side. A nose down twist of about 4° at ψ = 270° is shown. It must however be remembered that at this flight speed the whole span of the blade is in reversed flow so this twist is an aerodynamic increase in incidence here. This twist is therefore helping to increase the lift in this region. The non-dimensional root torsional moment is shown in Figure 26. The maximum value at 260 knots is similar to but has the opposite sign to that calculated for 160 knots, the maximum value at 340 knots is larger than the 160 knot value but in the same sense.

In summary the interpretation of the calculations made in this section suggests that:

The dynamic design of the rotor for the reversed flow circulation controlled high speed rotor involves similar compromises to those faced when designing a conventional edgewise rotor. The semi-rigid head has limited the blade flapping to

acceptable values. The maximum twist of the blade at a speed of 340 knots is significant and this is likely to be the limiting speed factor. The improvements which may be expected from a dedicated design of head and blade need to be investigated before any firm conclusion on the potential maximum speed can be reached.

7.0 CONCLUSIONS

1. The application of circulation control by blowing to conventional aerofoil sections operating in reversed flow has been wind tunnel tested. It was found that, with reasonable lift/jet momentum efficiency, positive lift was generated at all negative angles of attack. The most negative value tested was -20°. The lift augmentation also extended to positive angles of attack. The wind tunnel tests used full scale blade chord models.

2. The free vortex modelling of circulation control jet flow proposed by the authors and R.V. Smith proved very helpful in determining the chordwise position of the blowing slot fitted to an RAE 9615 section.

3. A computer model of a helicopter rotor, which could use circulation control on the rotor blades in the reversed flow region, was developed. The blade flapping was modelled in detail and a computer efficient technique was developed based on a harmonic method of solution. This model was used both for an isolated rotor in forward flight and, in conjunction with fuselage data, to trim a complete helicopter up to speeds of 340 knots. In both cases the model used had a Westland Lynx-like configuration. For the performance work a rigid rotor blade with offset flapping hinge model was used.

4. The calculations mentioned in 3. gave a performance up to $\mu = 0.4$ which agreed closely with real Lynx data. Above that advance ratio auxilliary thrust and circulation control were applied and the rotor progressively tilted backward towards autorotative flight. The rotor tip speed was reduced to maintain a maximum advancing tip Mach number of 0.95. Fuselage tilt was found to be acceptable. The rotor flapping at 340 knots was considered excessive.

5. The circulation control air compression power was found to be small. The rotor power also decreased to about zero at the high speeds.

6. The rotor performance could be most improved at the highest speed by the generation of increased lift on the advancing blade and at the front and rear of the disc. This suggests that the choice of aerofoil section(s) and blade geometry may produce significant improvements in overall performance relative to the figures quoted here.

7. The auxilliary thrust power dominated the total power required. At the cruise speeds of interest, namely 300--340 knots, the auxilliary thrust required exceeded the fuselage drag by about 26%. The fact that the fuselage data used related to a helicopter not designed for these high speeds meant that the high power figures calculated here would be reduced, nearly pro-rata, for a suitable high speed, lower drag fuselage.

8. The trimmed rotor thrust was a minimum at about $\mu = 0.8$. The transition through to higher speeds was eased by the availability of fuselage lift. The aerodynamic design of the fuselage with reference to lift and pitching moment while retaining a suitable operational shape, justifies further research.

9. The position and direction of the auxilliary thrust have not been investigated to date. These variables appear to have the potential to significantly improve the complete vehicle performance over that given in this paper.

10. The effect of allowing elastic freedoms in flap and torsion for the blades was investigated. Modelling the semi-rigid hub, typical of the Lynx but excluding any blade pre-cone angle, dramatically reduced the blade flapping to an acceptable value. The elastically bladed rotor was slightly easier to trim than its rigid counterpart. The performance in terms of power etc. was almost unaffected. The maximum non-dimensional blade flapping and torsion moment increased at the highest speed and these values are likely to be the limiting speed factors. The semi-rigid hub appears to be the preferred design but more extensive studies need to be made before that conclusion can be confirmed.

11. The fact that dimensions, structural properties and basic aerodynamic performance of blade sections and fuselage of an existing helicopter could be used to demonstrate that Reversed Flow Circulation Control was capable of producing a trimmed helicopter up to 340 knots suggests that the technique is robust. Furthermore for a dedicated design the performance suggested in this paper should be exceeded.

12. The calculations in this paper, when considered with the considerable earlier work in the UK first and then much more extensively in the USA later makes it reasonable to suggest that the technology now exists to design a 300 knot cruise and 340 knot dash speed edgewise rotor vehicle. Such a machine can take full advantage of all the conventional edgewise rotor design, construction and operational knowledge while offering the benefits of a much higher cruise speed.

8.0 REFERENCES

1. I.C. Cheeseman and A.R. Seed, The application of circulation control by blowing to helicopter rotors, **JRAeS** 71, 1967

2. V.E. Lockwood, Lift generation on a circular cylinder by tangential blowing from surface slots, **NASA TN** D-244, 1960.

3. K.R. Reader, D.G. Kirkpatrick and R.M. Williams, Status report on advanced development program utilizing circulation control rotor technology, **Proceedings of the 4th. European Rotorcraft and Powered Lift Forum, Stresa**, Paper No. 44 Sept. 1978.

4. W.A. Welsh and R.H. Blackwell, Higher harmonic and trim control of X-wing circulation control wind tunnel model rotor, **Proceedings of the 45th. AHS Forum,** 1990.

5. I.C. Cheeseman, Circulation control and its application to stopped rotor aircraft, **JRAeS** 72, 1968.

6. H. Tadghihi and T.L. Thompson, 'Notar', circulation control tail boom aerodynamic prediction and validation, **Proceedings of the 45th. AHS Forum**, 1990.

7. I.M. Davidson and T.J. Hargest, Helicopter noise, **JRAeS** 69, 1965.

8. E.O.Rogers, Recent progress in performance prediction of high advance ratio circulation controlled rotors, **Proceedings of the 6th. European Rotorcraft and Powered Lift Forum, Bristol**, Paper No 29, Sept. 1980.

9. I.C. Cheeseman, Developments in rotary wing aircraft aerodynamics. **Proceedings of the 7th. European Rotorcraft and Powered Lift Forum, Garmish Partenkirchen,** Paper No 1, 1981.

10. M.M.E.Soliman, R.V.Smith and I.C. Cheeseman, Modelling circulation control by blowing, **AGARD conference preprint CPP-355**, 1984.

9.0 ACKNOWLEDGEMENTS

The authors are pleased to take this opportunity to acknowledge the contractual support of (in alphabetical order) the Ministry of Defence, the Science and Engineering Research Council and Westland Helicopters Ltd. They have much appreciated the help and advice received from many people but chiefly from Peter Wilby and Alan Jones of the Royal Aerospace Establishment and David Balmford and David Humperson of Westland Helicopters Ltd. The assistance of their colleagues within the Department of Aeronautics and Astronautics at the University of Southampton is also gratefully acknowledged among whom the following deserve special mention: the late Mr. D.S. Stanton and Mr. N. Powell who oversaw the wind tunnel model construction and testing. Special thanks to Mrs C Pinnington for the typing and preparation of the paper.

Whilst acknowledging the help received from many colleagues and friends they wish to make it clear that they take full responsibility for all the conclusions.